

Fig. S1. DNA content and cell size of stationary phase and GD cells grown in YES medium and pairwise statistical data analysis. (A) DNA content in log phase, stationary phase, and GD cells. (B and C) Cell lengths (B) and volumes (C) of log phase, stationary phase, and GD cells. More than 50 cells were examined for each analysis. Lengths and volumes were measured at indicated time points after entry into stationary phase and/or transferring cells to YES-Glc medium. Lines indicate pairwise data sets with a non-significant difference ($P>0.05$ using the two-tailed

Student's *t*-test with the Bonferroni correction). Log: log phase cells; Stat: stationary phase cells; GD: GD cells. (D–I) Pairwise statistical analysis of data shown in Fig. 1B–E (D–G) and those shown in (B) and (C). *P*-values calculated using the two-tailed Student's *t*-test are shown. Upper and lower values indicate *P*-values before and after the Bonferroni correction, respectively. Table cells with yellow background indicate pairs with significant *P*-values after the Bonferroni correction.

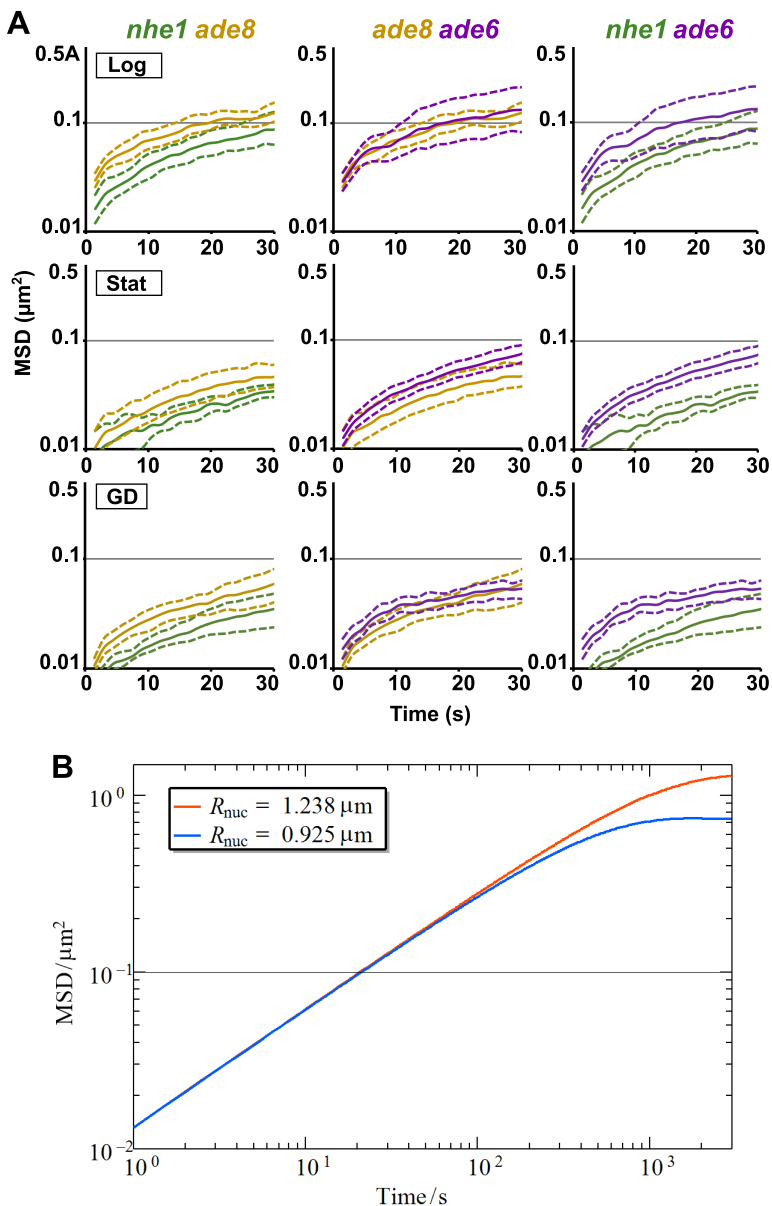


Fig. S2. Comparison of MSD plots of different chromosomal loci and MSD plots obtained from numerical simulations of a particle diffusing in the confined spaces. (A) Comparison of MSD plots described in Fig. 2E. (B) MSD plots obtained from numerical simulations of a particle diffusing in confined spherical spaces. The spaces reflect the observed nuclear sizes in log ($R_{\text{nuc}}= 1.238 \mu\text{m}$) and stationary ($R_{\text{nuc}}= 0.925 \mu\text{m}$) phases. The effect of the nuclear size on MSD is appreciable only when MSD exceeds $0.1 \mu\text{m}^2$, which is not in the observation range in Fig. 2D and reasonable for nuclear radii that are in the order of $1 \mu\text{m}$. Note that this simulation indicates that the repression of chromosome fluctuation cannot be simply attributed to the nucleus size-dependent spatial confinement. However, this does not exclude the possibility that nuclear size affects the chromosome fluctuation indirectly, i.e., nuclear shrinkage causes some changes in the intranuclear molecular composition through an uncharacterized biochemical mechanism, which lead to the repression of chromosome fluctuation.

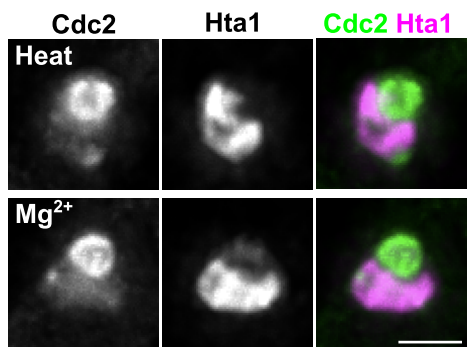


Fig. S3. Cdc2 localization in cells exposed to high temperature or high concentration of magnesium cation. Cells expressing GFP-tagged Cdc2 and mCherry-tagged Hta1 were exposed to 42°C for 20 min (Heat) or incubated in YES medium containing 0.5 M MgCl₂ for 2 hours (Mg²⁺). Scale bar, 2 μm.

Cell length @ 32°C		WT			cdc2-L7			Cell length @ 25°C		WT			cdc2			
		Stat 1 d	Log	Stat 1 d				WT	Log	Stat 1 d	Log	Stat 1 d				
WT	Log		8.9 x 10 ⁻¹² 5.3 x 10 ⁻¹¹		3.8 x 10 ⁻⁴ 2.3 x 10 ⁻³		3.7 x 10 ⁻¹	WT		7.4 x 10 ⁻⁷ 4.5 x 10 ⁻⁶		5.0 x 10 ⁻² 2.7 x 10 ⁻¹⁰		2.5 x 10 ⁻⁵ 1.6 x 10 ⁻⁹		
	Stat				4.5 x 10 ⁻¹³ 2.7 x 10 ⁻¹²		2.8 x 10 ⁻¹¹ 1.7 x 10 ⁻¹⁰					4.7 x 10 ⁻¹		1.5 x 10 ⁻⁴		
cdc2-L7	Log						6.3 x 10 ⁻³ 3.8 x 10 ⁻²	cdc2-L7	Log				1.2 x 10 ⁻⁷ 7.2 x 10 ⁻⁷			

Cell volume @ 32°C		WT			cdc2-L7			Cell volume @ 25°C		WT			cdc2-L7			
		Stat 1 d	Log	Stat 1 d				WT	Log	Stat 1 d	Log	Stat 1 d				
WT	Log		6.7 x 10 ⁻²⁵ 4.0 x 10 ⁻²⁴		1.4 x 10 ⁻¹³ 8.5 x 10 ⁻¹³		7.7 x 10 ⁻¹	WT		2.0 x 10 ⁻³⁷ 1.2 x 10 ⁻³⁶		4.4 x 10 ⁻¹ 6.9 x 10 ⁻⁴⁰		6.4 x 10 ⁻⁴⁶ 9.8 x 10 ⁻¹		
	Stat				3.1 x 10 ⁻²⁹ 1.8 x 10 ⁻²⁸		4.0 x 10 ⁻²⁴ 2.4 x 10 ⁻²³					4.2 x 10 ⁻³⁹		3.8 x 10 ⁻⁴⁵		
cdc2-L7	Log						7.2 x 10 ⁻¹³ 4.3 x 10 ⁻¹²	cdc2-L7	Log				3.6 x 10 ⁻⁴⁹ 2.2 x 10 ⁻⁴⁸			

Nuclear area @32°C		WT				cdc2-L7				
		Stat 0 d	Stat 1 d	-Glc 1 d	Log	Stat 0 d	Stat 1 d	-Glc 1 d		
WT	Log	2.8 x 10 ⁻⁵⁷ 7.8 x 10 ⁻⁵⁶	2.9 x 10 ⁻⁶³ 8.2 x 10 ⁻⁶²	2.4 x 10 ⁻³⁵ 6.7 x 10 ⁻³⁴	6.9 x 10 ⁻²² 1.9 x 10 ⁻²⁰	2.4 x 10 ⁻³ 6.9 x 10 ⁻²	3.0 x 10 ⁻³¹ 8.4 x 10 ⁻³⁰	7.6 x 10 ⁻¹⁰ 2.1 x 10 ⁻⁸		
	Stat 0 d		8.0 x 10 ⁻⁴ 2.2 x 10 ⁻²	2.3 x 10 ⁻¹⁹ 6.6 x 10 ⁻¹⁸	4.1 x 10 ⁻⁵⁷ 1.2 x 10 ⁻⁵⁵	7.9 x 10 ⁻³⁷ 2.2 x 10 ⁻³⁵	1.0 x 10 ⁻²⁰ 2.8 x 10 ⁻¹⁹	1.3 x 10 ⁻³² 3.7 x 10 ⁻³¹		
	Stat 1 d				1.8 x 10 ⁻²⁷ 5.1 x 10 ⁻²⁶	1.1 x 10 ⁻⁵¹ 3.1 x 10 ⁻⁶⁰	6.9 x 10 ⁻⁴³ 1.9 x 10 ⁻⁴¹	1.8 x 10 ⁻²⁸ 5.1 x 10 ⁻²⁷	3.0 x 10 ⁻³⁹ 8.4 x 10 ⁻³⁸	
	-Glc 1d					7.5 x 10 ⁻⁴⁷ 2.1 x 10 ⁻⁴⁵	3.5 x 10 ⁻¹⁸ 9.7 x 10 ⁻¹⁷	2.7 x 10 ⁻¹ 1.2 x 10 ⁻¹¹	1.2 x 10 ⁻¹¹ 3.2 x 10 ⁻¹⁰	
cdc2-L7	Log						3.9 x 10 ⁻²⁷ 1.1 x 10 ⁻²⁵	5.9 x 10 ⁻⁴⁶ 1.7 x 10 ⁻⁴⁴	9.1 x 10 ⁻³⁵ 2.6 x 10 ⁻³³	
	Stat 0 d							1.8 x 10 ⁻¹⁵ 4.9 x 10 ⁻¹⁴	5.4 x 10 ⁻³ 1.5 x 10 ⁻¹	
	Stat 1 d								4.8 x 10 ⁻⁹ 1.3 x 10 ⁻⁷	

Nuclear area @25°C		WT			cdc2-L7			
		Stat 0 d	Stat 1 d	-Glc 1 d	Log	Stat 0 d	Stat 1 d	-Glc 1 d
WT	Log	7.4 x 10 ⁻⁷¹ 2.1 x 10 ⁻⁶⁹	1.4 x 10 ⁻⁹⁸ 3.9 x 10 ⁻⁹⁷	6.8 x 10 ⁻⁵⁷ 1.9 x 10 ⁻⁵⁵	3.7 x 10 ⁻¹ 1.2 x 10 ⁻⁷³	4.4 x 10 ⁻⁷⁵ 1.1 x 10 ⁻⁹⁵	4.1 x 10 ⁻⁹⁷ 8.1 x 10 ⁻⁵⁷	2.9 x 10 ⁻⁵⁸ 8.1 x 10 ⁻⁵⁷
	Stat 0 d		1.2 x 10 ⁻⁴² 3.4 x 10 ⁻⁴¹	2.0 x 10 ⁻³⁹ 5.6 x 10 ⁻³⁸	1.5 x 10 ⁻⁶⁰ 4.1 x 10 ⁻⁵⁹	5.9 x 10 ⁻¹ 1.8 x 10 ⁻³⁹	2.9 x 10 ⁻⁵² 8.1 x 10 ⁻⁵¹	1.7 x 10 ⁻³⁹ 4.7 x 10 ⁻³⁸
	Stat 1 d				1.0 x 10 ⁻⁷⁶ 2.8 x 10 ⁻⁷⁵	5.7 x 10 ⁻⁸² 1.6 x 10 ⁻⁸⁰	6.4 x 10 ⁻⁴¹ 1.8 x 10 ⁻³⁹	7.3 x 10 ⁻¹ 4.1 x 10 ⁻⁷⁷
	-Glc 1d					2.2 x 10 ⁻⁴⁶ 6.3 x 10 ⁻⁴⁵	2.2 x 10 ⁻³⁴ 6.0 x 10 ⁻³³	3.6 x 10 ⁻⁸⁵ 1.0 x 10 ⁻⁸³
cdc2-L7	Log						1.9 x 10 ⁻⁶² 5.5 x 10 ⁻⁶¹	9.4 x 10 ⁻⁸¹ 2.6 x 10 ⁻⁷⁹
	Stat 0 d							1.5 x 10 ⁻⁴⁷ 4.2 x 10 ⁻⁴⁶
	Stat 1 d							4.9 x 10 ⁻³³ 1.4 x 10 ⁻³¹

Chromosome area @32°C		WT			cdc2-L7			
		Stat 0 d	Stat 1 d	-Glc 1 d	Log	Stat 0 d	Stat 1 d	-Glc 1 d
WT	Log	3.5 x 10 ⁻³⁸ 9.8 x 10 ⁻³⁷	2.7 x 10 ⁻⁴⁵ 7.5 x 10 ⁻⁴⁴	2.6 x 10 ⁻²⁹ 7.3 x 10 ⁻²⁸	6.4 x 10 ⁻¹⁴ 1.8 x 10 ⁻¹²	1.4 x 10 ⁻¹³ 4.0 x 10 ⁻¹²	5.3 x 10 ⁻²⁷ 1.5 x 10 ⁻²⁵	6.5 x 10 ⁻¹⁶ 1.8 x 10 ⁻¹⁴
	Stat 0 d		5.7 x 10 ⁻¹³ 1.6 x 10 ⁻¹¹	1.6 x 10 ⁻¹¹ 4.4 x 10 ⁻⁷	2.1 x 10 ⁻⁴⁴ 5.8 x 10 ⁻⁴³	6.7 x 10 ⁻²⁰ 1.9 x 10 ⁻¹⁸	7.3 x 10 ⁻¹¹ 2.1 x 10 ⁻⁹	3.2 x 10 ⁻²⁰ 9.1 x 10 ⁻¹⁹
	Stat 1 d			2.5 x 10 ⁻⁴³ 6.9 x 10 ⁻⁴²	2.1 x 10 ⁻⁴⁵ 5.8 x 10 ⁻⁴⁴	5.7 x 10 ⁻³³ 1.6 x 10 ⁻³¹	2.3 x 10 ⁻³⁹ 6.5 x 10 ⁻³⁸	9.2 x 10 ⁻³⁸ 2.6 x 10 ⁻³⁶
	-Glc 1d				5.3 x 10 ⁻³⁷ 1.5 x 10 ⁻³⁵	1.1 x 10 ⁻¹⁰ 3.0 x 10 ⁻⁹	7.7 x 10 ⁻² 1.8 x 10 ⁻⁸	6.4 x 10 ⁻¹⁰ 1.8 x 10 ⁻⁸
cdc2-L7	Log					2.4 x 10 ⁻³⁰ 6.7 x 10 ⁻²⁹	8.8 x 10 ⁻³⁷ 2.5 x 10 ⁻³⁵	6.1 x 10 ⁻³² 1.7 x 10 ⁻³⁰
	Stat 0 d						1.5 x 10 ⁻⁷ 2.0 x 10 ⁻⁶	5.2 x 10 ⁻¹
	Stat 1 d							1.5 x 10 ⁻⁶ 4.3 x 10 ⁻⁵

Chromosome area @25°C		WT			cdc2-L7			
		Stat 0 d	Stat 1 d	-Glc 1 d	Log	Stat 0 d	Stat 1 d	-Glc 1 d
WT	Log	4.4 x 10 ⁻³² 1.2 x 10 ⁻³⁰	9.4 x 10 ⁻⁵⁴ 2.6 x 10 ⁻⁵²	1.5 x 10 ⁻²¹ 4.1 x 10 ⁻²⁰	7.6 x 10 ⁻¹	6.4 x 10 ⁻²⁵ 1.8 x 10 ⁻²³	5.9 x 10 ⁻⁵⁴ 1.7 x 10 ⁻⁵²	3.6 x 10 ⁻²³ 1.0 x 10 ⁻²¹
	Stat 0 d		4.3 x 10 ⁻⁴⁶ 1.2 x 10 ⁻⁴⁴	1.4 x 10 ⁻¹⁰ 3.8 x 10 ⁻⁹	2.1 x 10 ⁻²⁶ 5.9 x 10 ⁻²⁵	2.8 x 10 ⁻⁴ 7.8 x 10 ⁻³	3.8 x 10 ⁻³³ 1.1 x 10 ⁻³¹	3.7 x 10 ⁻¹¹ 1.0 x 10 ⁻⁹
	Stat 1 d			2.1 x 10 ⁻⁶⁵ 5.8 x 10 ⁻⁶⁴	2.1 x 10 ⁻⁴⁶ 5.8 x 10 ⁻⁴⁵	1.2 x 10 ⁻⁴⁴ 3.2 x 10 ⁻⁴³	1.1 x 10 ⁻² 3.1 x 10 ⁻¹	2.8 x 10 ⁻⁶⁵ 7.8 x 10 ⁻⁶⁴
	-Glc 1d				3.9 x 10 ⁻¹⁷ 1.1 x 10 ⁻¹⁵	2.0 x 10 ⁻² 5.6 x 10 ⁻¹	3.5 x 10 ⁻⁴⁷ 9.8 x 10 ⁻⁴⁶	4.0 x 10 ⁻¹
cdc2-L7	Log					2.4 x 10 ⁻²⁰ 6.6 x 10 ⁻¹⁹	1.8 x 10 ⁻⁴⁶ 4.9 x 10 ⁻⁴⁵	1.5 x 10 ⁻¹⁸ 4.2 x 10 ⁻¹⁷
	Stat 0 d						5.1 x 10 ⁻³⁶ 1.4 x 10 ⁻³⁴	6.0 x 10 ⁻²
	Stat 1 d							8.9 x 10 ⁻⁴⁴ 2.5 x 10 ⁻⁴²

Nuclear vol @32°C		WT		cdc2-L7		N/C ratio @32°C		WT		cdc2-L7		
		Stat 1 d	-Glc 1 d	Log	Stat 1 d	-Glc 1 d	Stat 1 d	-Glc 1 d	Log	Stat 1 d	-Glc 1 d	
WT	Log	5.7 x 10 ⁻⁴⁹ 8.6 x 10 ⁻⁴⁸	2.4 x 10 ⁻³⁰ 6.7 x 10 ⁻³⁴	6.3 x 10 ⁻¹⁷ 9.5 x 10 ⁻¹⁶	7.4 x 10 ⁻²⁷ 1.1 x 10 ⁻²⁵	1.9 x 10 ⁻¹⁰ 2.8 x 10 ⁻⁹	WT	5.3 x 10 ⁻²⁶ 8.0 x 10 ⁻²⁵	5.8 x 10 ⁻²⁹ 8.8 x 10 ⁻²⁸	7.7 x 10 ⁻¹	1.5 x 10 ⁻²³ 2.2 x 10 ⁻²²	1.2 x 10 ⁻²⁹ 1.8 x 10 ⁻²⁸
	Stat 1 d		3.6 x 10 ⁻²⁹ 7.5 x 10 ⁻²⁶	1.2 x 10 ⁻³⁹ 1.8 x 10 ⁻³⁸	1.6 x 10 ⁻²⁸ 2.4 x 10 ⁻²⁷	3.9 x 10 ⁻³⁵ 5.8 x 10 ⁻³⁴		4.1 x 10 ⁻² 6.1 x 10 ⁻¹	2.5 x 10 ⁻²⁴ 3.8 x 10 ⁻²³	3.1 x 10 ⁻¹	1.0 x 10 ⁻² 1.5 x 10 ⁻¹	
	-Glc 1d			9.3 x 10 ⁻³³ 1.4 x 10 ⁻³¹	1.1 x 10 ⁻¹	2.2 x 10 ⁻¹¹ 3.3 x 10 ⁻¹⁰			4.0 x 10 ⁻²⁷ 6.0 x 10 ⁻²⁶	7.6 x 10 ⁻³ 1.1 x 10 ⁻¹		4.8 x 10 ⁻¹
cdc2-L7	Log				4.1 x 10 ⁻³² 6.2 x 10 ⁻³¹	1.3 x 10 ⁻²⁶ 2.0 x 10 ⁻²⁵	cdc2-L7			2.1 x 10 ⁻²² 3.1 x 10 ⁻²¹		5.0 x 10 ⁻²⁸ 7.5 x 10 ⁻²⁷
	Stat 1 d					6.1 x 10 ⁻⁸ 9.1 x 10 ⁻⁷		Stat 1 d				1.6 x 10 ⁻³ 2.3 x 10 ⁻²

Nuclear vol @25°C		WT		cdc2-L7		N/C ratio @25°C		WT		cdc2-L7		
		Stat 1 d	-Glc 1 d	Log	Stat 1 d	-Glc 1 d	Stat 1 d	-Glc 1 d	Log	Stat 1 d	-Glc 1 d	
WT	Log	1.4 x 10 ⁻⁵⁶ 2.0 x 10 ⁻⁵⁵	7.2 x 10 ⁻⁴¹ 1.1 x 10 ⁻³⁹	4.6 x 10 ⁻¹	2.0 x 10 ⁻⁵⁵ 2.9 x 10 ⁻⁵⁴	5.6 x 10 ⁻³⁸ 8.4 x 10 ⁻³⁷	WT	3.1 x 10 ⁻¹⁴ 4.7 x 10 ⁻¹³	1.7 x 10 ⁻²² 2.6 x 10 ⁻²¹	9.4 x 10 ⁻¹	1.4 x 10 ⁻²³ 2.1 x 10 ⁻²²	1.4 x 10 ⁻²⁷ 2.1 x 10 ⁻²⁶
	Stat 1 d		1.9 x 10 ⁻³⁷ 2.9 x 10 ⁻³⁶	6.8 x 10 ⁻⁵² 1.0 x 10 ⁻⁵⁰	6.2 x 10 ⁻¹	2.8 x 10 ⁻⁴² 4.2 x 10 ⁻⁴¹		3.9 x 10 ⁻² 5.9 x 10 ⁻¹	3.6 x 10 ⁻¹¹ 5.4 x 10 ⁻¹⁰	7.0 x 10 ⁻¹	1.2 x 10 ⁻² 1.8 x 10 ⁻¹	
	-Glc 1d			1.4 x 10 ⁻³⁷ 2.0 x 10 ⁻³⁶	2.2 x 10 ⁻³⁵ 3.3 x 10 ⁻³⁴	1.9 x 10 ⁻¹			2.6 x 10 ⁻¹⁷ 3.9 x 10 ⁻¹⁶	3.3 x 10 ⁻² 5.0 x 10 ⁻¹	8.2 x 10 ⁻¹	
cdc2-L7	Log				5.4 x 10 ⁻⁵¹ 8.1 x 10 ⁻⁵⁰	2.1 x 10 ⁻³⁵ 3.2 x 10 ⁻³⁴	cdc2-L7			3.2 x 10 ⁻¹⁵ 4.7 x 10 ⁻¹⁴		7.9 x 10 ⁻²⁰ 1.2 x 10 ⁻¹⁸
	Stat 1 d					1.2 x 10 ⁻⁴¹ 1.8 x 10 ⁻⁴⁰		Stat 1 d				4.3 x 10 ⁻³ 6.5 x 10 ⁻²

Nuclear vol ± analog	DMSO 4h	DMSO 1 d	3MB- PP1 4h	3MB- PP1 1d	NC ratio ± analog	DMSO 4h	DMSO 1 d	3MB- PP1 4h	3MB- PP1 1d
Log	8.6×10^{-33} 8.6×10^{-32}	3.6×10^{-43} 3.6×10^{-42}	1.1×10^{-4} 1.1×10^{-3}	2.1×10^{-18} 2.1×10^{-19}	Log	1.9×10^{-10} 1.0×10^{-9}	3.4×10^{-22} 3.4×10^{-21}	7.6×10^{-1}	3.3×10^{-10} 3.3×10^{-9}
DMSO 4h		1.4×10^{-9} 1.4×10^{-8}	6.3×10^{-19} 6.3×10^{-18}	2.5×10^{-3} 2.5×10^{-2}	DMSO 4h		1.3×10^{-6} 1.3×10^{-5}	4.2×10^{-10} 4.2×10^{-9}	3.0×10^{-1}
DMSO 1 d			1.6×10^{-27} 1.6×10^{-26}	2.2×10^{-11} 2.2×10^{-10}	DMSO 1 d			3.5×10^{-21} 3.5×10^{-20}	1.1×10^{-9} 1.1×10^{-8}
3MB- PP1 4h				3.2×10^{-9} 3.2×10^{-8}	3MB- PP1 4h				1.2×10^{-9} 1.2×10^{-8}

Fig. S4. Pairwise statistical analysis of data shown in Fig. 5 and S5. *P*-values calculated using two-tailed Student's *t*-test are shown. Upper and lower values indicate *P*-values before and after the Bonferroni correction, respectively. Table cells with yellow background indicate pairs with significant *P*-values after the Bonferroni correction.

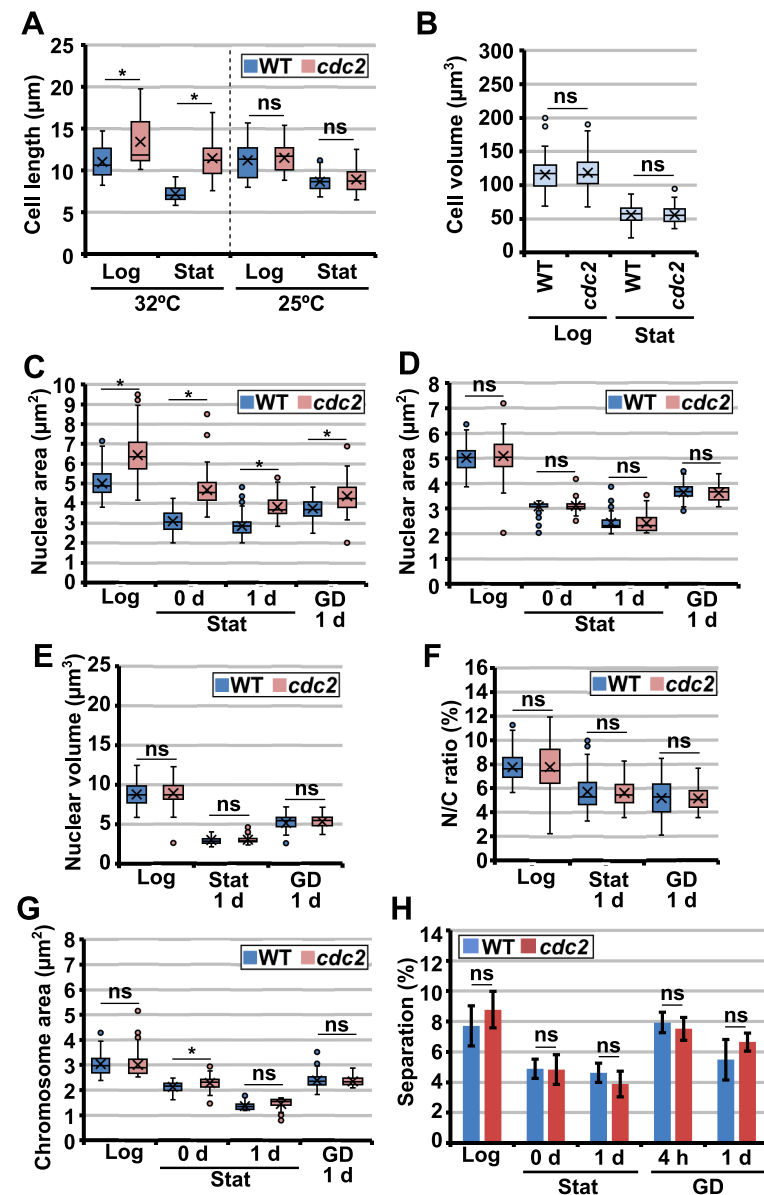


Fig. S5. The effects of *cdc2* temperature-sensitive mutation on the cell state. (A) Lengths of wild-type and *cdc2*-L7 cells in log and stationary phases. Thirty cells were examined for each analysis. (B) Volumes of wild-type and *cdc2*-L7 cells in log and stationary phases at 25°C. (C and D) Areas of the nuclei in wild-type and *cdc2*-L7 cells at 32°C (C) and 25°C (D). (E and F) Nuclear volumes in wild-type and *cdc2*-L7 cells (E) and their N/C ratios (F) at 25°C. (G) Areas of chromosome-occupying spaces in wild-type and *cdc2*-L7 cells at 25°C. In (B) to (G), more than 50 cells were examined for each analysis. (H) Sister locus separation in wild-type and *cdc2*-L7 cells at 25°C. More than 100 cells were examined for each analysis, and bars indicate the mean values from three independent experiments. Error bars: S. E. M. Only statistical comparisons between wild-type and *cdc2*-L7 cells are shown. *: significant; ns: not significant. Statistical analyses were carried out using the unpaired, two-tailed Student's *t*-test with the Bonferroni correction (Fig. S4).

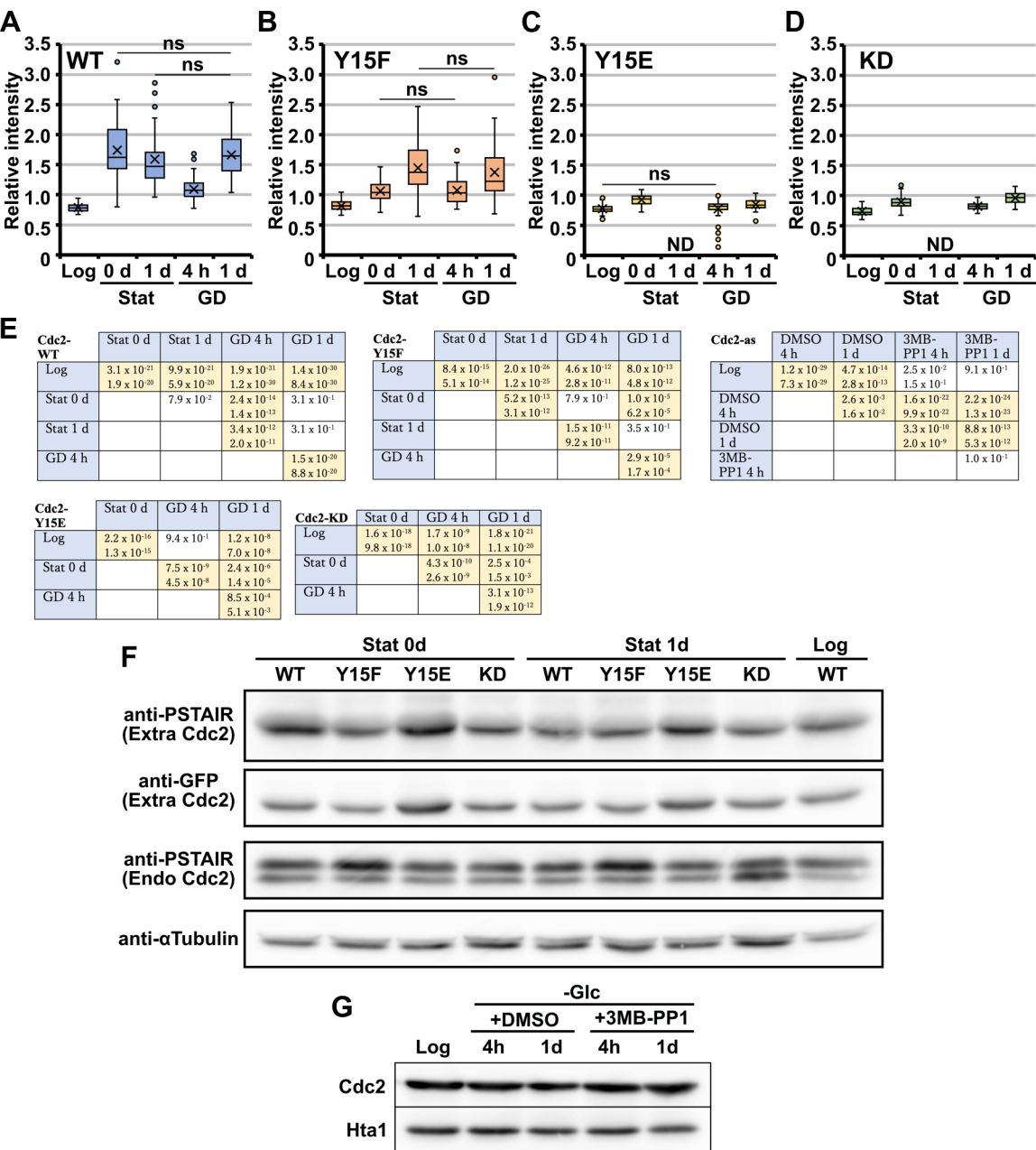


Fig. S6. Signal intensities of Cdc2 variants in the nucleolar region relative to those in the chromosomal region and protein levels of Cdc2 variants. (A–D) Relative signal intensities of wild-type Cdc2 (A), Cdc2-Y15F (B), Cdc2-Y15E (C), and Cdc2-KD (D) in the nucleolar region. More than 40 cells were examined for each analysis. Only pairwise data sets with a non-significant difference ($P>0.05$) are shown. ND: not determined. (E) P -values of pairwise data sets shown in (A) to (D) and Fig. 7C. The P -values were calculated using the two-tailed Student's t -test (upper values) and corrected by the Bonferroni correction (lower values). In the table, the yellow background indicates pairs with significant P -values after the Bonferroni correction. (F) Protein levels of the phosphorylation-mutant forms of Cdc2. (G) The protein level of Cdc2-as in GD cells. Cdc2 and Hta1 were detected by anti-PSTAIR and anti-GFP antibodies, respectively. +DMSO: in the presence of DMSO; +3MB-PP1: in the presence of 3MB-PP1.

Table S1. Strain List

Strain name	Genotype	Figs
SMHT16-1	$h^+ lysI^+::ccrl-N-GFP htaI^+::mCherry-nat^R$	1A–E, 5D–G, 8A–D, S1C–G, S1I, S4, S5B–G
SMH27-8D	$h^- leuI-32 ura4-D18 nheI^+::kan^R-ura4^+-lacO aurI^+::aurI^R-Pnda3-GFP-lacI lysI^+::Pnda3-mCherry-atb2^+$	2C, 2E, S2A
SMHT5-1	$h^- leuI-32 ura4-D18 ade8::kan^R-ura4^+-lacO aurI^+::aurI^R-Pnda3-GFP-lacI lysI^+::Pnda3-mCherry-atb2^+$	2C–E, S2A
SMHT6-1	$h^- leuI-32 ura4-D18 ade6::kan^R-ura4^+-lacO aurI^+::aurI^R-Pnda3-GFP-lacI lysI^+::Pnda3-mCherry-atb2^+$	2B, 2C, 2E, 5H, 5I, S2A, S5H
SMH2-9B	$h^+ cdc2^+::GFP-kan^R htaI^+::mCherry-nat^R$	3A, 3B, S3
SKY31-13A	$h^+ leuI-32? cdc13^+::GFP-LEU2 aurI^+::aurI^R-Pcdc2-cdc2^+-mCherry$	3C
SKY23-1A	$h^+ lysI^+::Pclp1-clp1^+-GFP aurI^+::aurI^R-Pcdc2-cdc2^+-mCherry$	3C
SKY22-3A	$h^+ leuI-32 aurI^+::aurI^R-Pgar1-gar1^+-mCherry cdc2^+::GFP-kan^R$	3C
SKY33-6C	$h^+ gar2^+::mCherry-kan^R cdc2^+::GFP-kan^R$	3C
L972	h^-	4A–C, 5A–C, S1A, S1B, S1H, S4, S5A
SMH17-1C	$h^- cdc2-L7$	5A–C, S4, S5A
SMH23-1D	$h^+ cdc2-L7 lysI^+::ccrl-N-GFP htaI^+::mCherry-nat^R$	5D–G, 8A–D, S4, S5B–G
SMH13-6C	$h^+ lysI^+::ccrl-N-GFP aurI^+:: aurI^R-Pcdc2-cdc2as-mCherry cdc2::nat^R htaI^+::GFP-nat^R$	5J, 5K, S4
SMH26-1C	$h^- leuI-32 ura4-D18 cdc2-L7 ade6::kan^R-ura4^+-lacO aurI^+::aurI^R-Pnda3-GFP-lacI lysI^+::Pnda3-mCherry-atb2^+$	5H, 5I, S5H
SKY25-9A	$h^- aurI^+:: aurI^R-Pcdc2-cdc2^+-GFP htaI^+::mCherry-nat^R$	6B, 6C, S6A, S6E, S6F
SKY30-9A	$h^- aurI^+:: aurI^R-Pcdc2-cdc2-Y15F-GFP htaI^+::mCherry-nat^R$	6B, 6C, S6B, S6E, S6F
SKY27-3C	$h^- aurI^+:: aurI^R-Pcdc2-cdc2-Y15E-GFP htaI^+::mCherry-nat^R$	6B, 6C, S6C, S6E, S6F
SKY26-13D	$h^- aurI^+:: aurI^R-Pcdc2-cdc2-KD-GFP htaI^+::mCherry-nat^R$	6B, 6C, S6D–F
SYN38-4D	$h^- aurI^+:: aurI^R-Pcdc2-cdc2as-mCherry cdc2::nat^R htaI^+::GFP-nat^R$	7A–C, 8E, S6E, S6G

Table S2. Primer list

Use	Primer sequence
Construction of the <i>htal-mCherry</i> fusion	TTAATTAAACCCGGGATCCGTGAGCGTTCGCCACGGAGAC
	CCGGAGGTGTTAAGAACGCT
	GTTTAAACGAGCTGAATTCCCTCAGGACTTTGGCAATTGT
	AAACTTGTCACTCTCAAGGCTG
Construction of the <i>clp1-mCherry</i> fusion	AGAGATCTGGTATATCGCTGTAACAGCG
	AGAGATCTTAGAAATTAGCCGGCTTTAGAAG
	ACGCGTCGACGAAGATCTCGGATCCCCGGGTTAATTAAC
	GGGGTACCATATTACCCTGTTATCCCTAGCG
Construction of <i>cdc2-mCherry</i> and -GFP fusions	TCCGAGCTCGCTGTTCCCTAGTAATAGTTATTA
	ACGCGTCGACTGCAAACCACTAAAAGAAGCAAC
	ACGCGTCGACATGGAGAATTATCAAAAAGTCGAAA
	CGGGATCCCATGAAAATCACGAAGATAATTTGTT
	ACGCGTCGACGAAGATCTCGGATCCCCGGGTTAATTAAC
	CAAACAGGAATCGAATGCAACC
Generation of <i>cdc2-as</i> mutation	GGTGAGTTTTAGACATGGATTGAAAAAAAT
	AACAAGATAAAGCTTGATTCACTGTAAA
Generation of <i>cdc2-Y15F</i> mutation	TGGCGTTGTTATAAAGCAAGACATAA
	AAGGTACCCAATTTTCGACTTTGATAATT
Generation of <i>cdc2-Y15E</i> mutation	GAAGGC GTT GTT ATA AAG CAAG ACATA AA
	CGTT CCTT CCCC AATT T TCG ACT TTTG
Generation of <i>cdc2-KD</i> mutation	CGAAAAATT CGC TTGAAG ATGAAT CTGAG
	CATCGCGACAATA CGCC CTGACA ATT T